CHALMERS

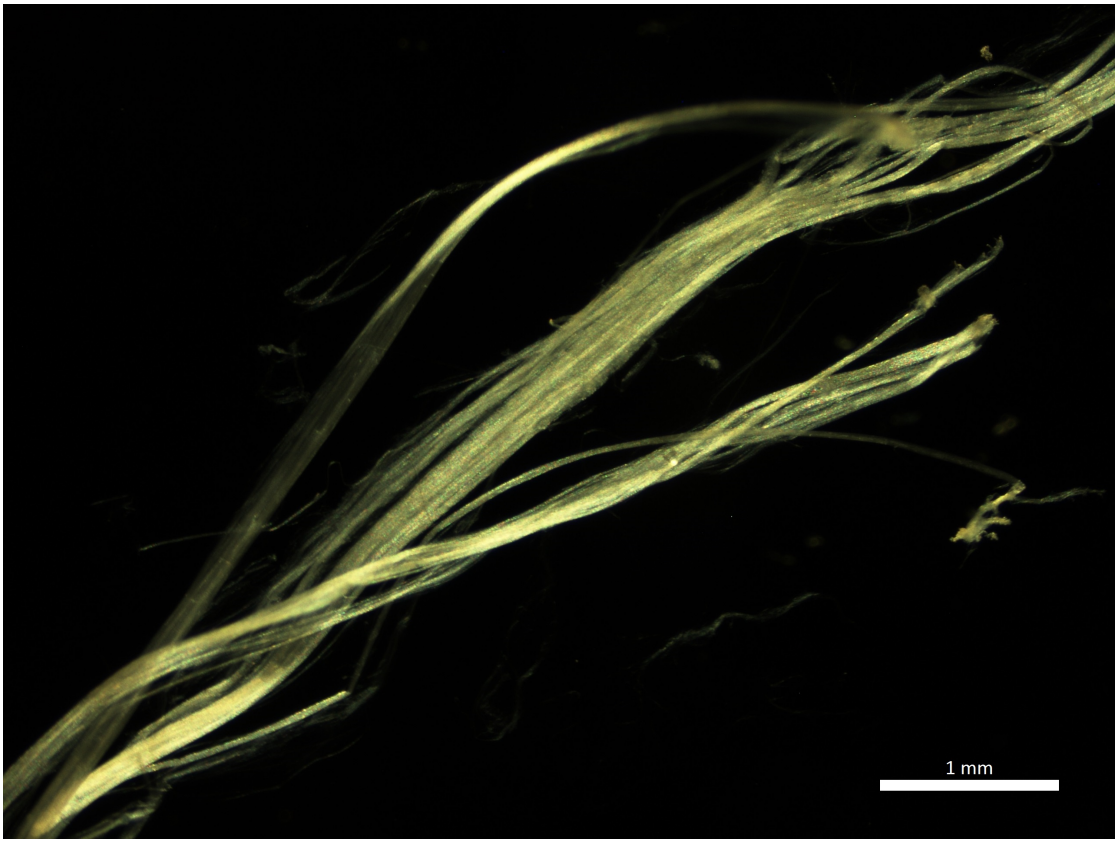

Antimicrobial silk

Master's Thesis in Biology and Biological Engineering

LOTTA SAVONEN FLODERUS

Department of Biology & Biological Engineering
Chalmers University of Technology
Gothenburg, Sweden, 2016

Master's thesis 2016

Antimicrobial silk

LOTTA SAVONEN FLODERUS

CHALMERS
UNIVERSITY OF TECHNOLOGY

Department of Biology & Biological Engineering
Chalmers University of Technology
Gothenburg, Sweden 2016

Antimicrobial silk
LOTTA SAVONEN FLODERUS

Master's Thesis 2016:NN
Department of Biology & Biological Engineering
Chalmers University of Technology
SE-412 96 Gothenburg
Sweden

Abstract

Spider silk has shown potential for use as a biomaterial. If fused to antimicrobial peptides (AMPs), recombinant spider silk could be used for medical applications and reduce the need to use conventional antibiotics to battle infections. Recombinant spider silk 4RepCT was fused to the AMPs Magainin I, Lactoferricin and a synthetically derived AMP referred to as WGR. Polystyrene disks were coated with the AMP-silk fusion proteins and the disks were incubated with cultures of *Staphylococcus aureus* and *Escherichia coli*, to test the AMP-silks antimicrobial activity. All AMP-silk fusion proteins significantly decreased bacterial adhesion of *S. aureus* to the disks after 48 hours of incubation compared to uncoated disks. The Mag- and WGR-silks were effective already after 24 hours. The recombinant silk itself seemed to have an antimicrobial effect by reducing bacterial adhesion of both bacterial strains to the polystyrene disks. Results indicated that addition of the AMPs improved this effect on *S. aurues*, but not on *E. coli*.

Acknowledgements

I would like to thank my supervisor at KTH, Linnea Nilebäck, for patiently and pedagogically teaching me everything I needed to know to overcome this task. The same goes for my supervisors at SP, Annika Krona and Lisbeth Märs. Thank you for your guidance at the confocal microscope and in the laboratory. And Erik Nygren, for answering questions about everything growing. My gratitude extends to everyone at KTH level 3 and the Microbiology- and Structure- departments at SP for making me feel welcome during my stay there. Thank you, Joakim Norbeck, for accepting the task of examining this diploma work, even during the initial fuss of getting it accepted into the student portal without having to hand in a physical copy of the initiation form. Family and friends, thank you for your care and support. A special thanks to Jackson for waking me up in the mornings (by stepping on my face). And most importantly to Jonas - For providing purpose.

Lotta Savonen Floderus

Contents

1 Introduction **1**
- 1.1 Antimicrobial spider silk . . . 2
- 1.2 Objective . . . 2
- 1.3 Delimitations . . . 3

2 Theory **4**
- 2.1 Spider silk . . . 4
  - 2.1.1 Using recombinant spider silk as a biomaterial . . . 5
- 2.2 Antimicrobial peptides . . . 5
  - 2.2.1 Target mechanism and antimicrobial activity . . . 6
  - 2.2.2 Using antimicrobial peptides for medical applications . . . 8
- 2.3 Infectious bacteria . . . 10
  - 2.3.1 Biofilm formation . . . 11
  - 2.3.2 Commonly encountered infectious bacteria . . . 11
- 2.4 Confocal laser scanning microscopy . . . 12

3 Materials and Methods **13**
- 3.1 Protein production and purification . . . 13
  - 3.1.1 Purification of WGR-silk fusion protein . . . 14
  - 3.1.2 Evaluation of purified WGR-silk fusion protein functionality . . . 14
- 3.2 Preparation of disks for antimicrobial activity assays . . . 14
- 3.3 Antimicrobial activity assays . . . 15
  - 3.3.1 Strains and overnight cultures . . . 15
  - 3.3.2 Colony forming units . . . 15
  - 3.3.3 Confocal laser scanning microscopy . . . 16
- 3.4 Statistical analysis . . . 18

4 Results **19**
- 4.1 Purification and function of WGR-silk fusion protein . . . 19
- 4.2 Antimicrobial activity assays . . . 21
  - 4.2.1 Colony forming units . . . 21
  - 4.2.2 Confocal laser scanning microscopy . . . 22

5 Discussion **27**
5.1 Purification efficiency of WGR-silk fusion protein 27
5.2 Evaluation of the antimicrobial activity assays 28
5.2.1 Evaluation methods not suitable for *P. aeruginosa* 29
5.2.2 Large variation between replicates in CFU-trials 29
5.2.3 Sonication procedure had a positive effect on bacteria viability . . 30
5.2.4 Alternative method for CFU-trials 30
5.2.5 AMP-silks' efficiency differed between species of bacteria 31
5.2.6 AMP-silks influenced biofilm formation 31
5.2.7 Only the living fractions of bacteria were compared 32
5.2.8 Weaker adhesion of bacteria on uncoated disks 33
5.2.9 Image analysis of investigated disks 33

6 Conclusions **34**

7 Future work **35**

References **36**

1

Introduction

The conventional use of antibiotics to battle infections is a growing problem, as strains of resistant bacteria keep developing [1]. Such strains are unaffected by traditional antibiotics and are therefore posing a great threat to modern society, where common diseases caused by resistant bacteria would no longer be easily treatable. Alternatives to traditional antibiotics is becoming more urgent and the research in this field is growing [2–5]. One alternative to traditional antibiotics could be to use antimicrobial peptides (AMPs), which are short chains of amino acids with a bactericidal effect. Antimicrobial peptides are produced for this purpose as part of the innate immune system in many life forms, and often have a broad spectrum of bactericidal activity. AMPs seem to have a more general targeting of the bacterial cell membranes than conventionally used antibiotics, which often have a specific binding site or target mechanism on the microbes. Bacteria can undergo mutations, altering the configuration of these specific target sites and thereby develop resistance to conventional antibiotics. More radical changes of the bacterial membrane configuration would likely be required for resistance development towards AMPs. Using AMPs instead of conventional antibiotics could therefore constrain resistance development towards antibiotics in bacteria and serve as a functional antimicrobial agent towards already resistant strains.

Combining the effect of antimicrobial peptides with properties of other materials could enable the development of novel biomaterials for medical applications. One candidate that has shown promising result as a strong and versatile biocompatible material is spider silk [6, 7]. Recombinant spider silk proteins can be expressed as fusion proteins together with different functional motifs or domains using a bacterial cloning host [8, 9]. This makes recombinant spider silk a potential starting material for a variety of applications [6–11]. In this study, the functionalization of the produced biomaterial is focused towards an antimicrobial effect, using different AMPs fused to the recombinant spider silk 4RepCT. The fusion proteins have been produced in a strain of *Escherichia coli*, and the resulting functionalized spider silk proteins showed ability to form fibers after purification [8].

1.1 Antimicrobial spider silk

A previous study on silk protein fused to antimicrobial peptides showed potential for this application as an alternative to conventional antibiotics [3]. In that study, another type of recombinant silk protein was used and fused to three different AMPs. They found an antimicrobial effect of the tested AMP-silks on *E. coli* and *S. aureus* [3]. The antimicrobial effect was however not investigated for any solid format of the AMP-silk proteins, which is the desirable form for many medical applications, such as coatings of implants.

An advantage of using recombinant spider silk fused to AMPs, over other antimicrobial coatings, is the silk's intrinsic ability to assemble into coatings and other formats, in physiological-like conditions [7]. This saves time compared to other methods, where additional preparation steps are needed for coating [12]. The ability to use standardized methods and a well known expression organism, such as *E. coli*, for expression of the AMP-silks, is advantageous when scaling up production and would increase the possibility for AMP-silks to be an available alternative to conventional antibiotics.

1.2 Objective

The aim of this diploma work was to evaluate the antimicrobial properties of antimicrobial peptides fused to recombinant spider silk. The antimicrobial properties of recombinant spider silk protein 4RepCT, fused to one of the AMPs Magainin I (Mag), Lacroferricin (Lac) or a peptide sequence thought to be optimized for antimicrobial effect, referred to as WGR, were tested on commonly encountered infectious bacteria. One bacterial strain of *Escherichia coli*, one strain of *Pseudomonas aeruginosa* and one strain of *Staphylococcus aureus* were used in antimicrobial assays, as they are often causing infections in hospital environments [13]. The species were also chosen due to their difference in cell wall configuration, where the first two are Gram-negative and the last is Gram-positive. The antimicrobial assays investigated if the AMP-silk proteins had an antimicrobial effect when adhered to a surface and if that effect differed between species of bacteria.

A secondary objective was to purify the WGR-silk fusion protein, evaluate the purification procedure, as well as determine the functionality of the purified construct.

1.3 Delimitations

In this study, three different antimicrobial peptides that have previously been cloned along with the spider silk protein were investigated [8]. The peptides were chosen after availability and might not have been optimal for the bacteria most relevant in a hospital environment. The purpose in this project was mainly to test if the AMP-silk proteins had a bactericidal effect when adhered to a surface, not to optimize this effect against relevant bacteria or to find optimal antimicrobial peptides for this purpose.

2

Theory

This section will explain the concepts of importance to this thesis work, beginning with a more detailed description of the spider silk protein and antimicrobial peptides. It will also give a short introduction to the bacteria that were used to test the antimicrobial effect of the recombinant spider silk fusion proteins, ending with the theory behind the microscopy method that was used to study them.

2.1 Spider silk

Spider silk is a very strong and elastic material that is showing potential as a biomaterial for medical use, since it is both biocompatible and readily accessible for bioengineering [7]. The native form of spider silk protein, also called spidroins, consists of a non-repetitive N-terminal domain, followed by repetitive glycine and alanine rich regions and a non-repetitive folded C-terminal domain (Fig. 2.1, left) [7]. It is the region of long repetitive sequences which is thought to contribute to the silk's stability and elasticity after assembly [14].

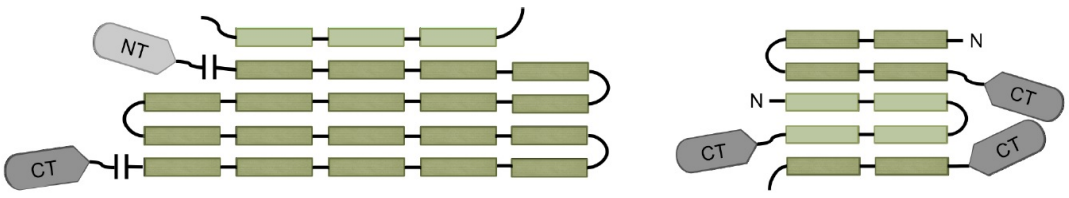

Figure 2.1: Schematic representations of suggested stacking of native spider silk (left) and the recombinant spider silk 4RepCT (right). [8]

2.1.1 Using recombinant spider silk as a biomaterial

Production of recombinant spider silk which tries to mimic the amount of long repetitive sequence of the native form has shown problems including genetic instability, unwanted mRNA secondary structures, deprived tRNA pool and solubility issues and proteolysis of the expressed protein [7]. These problems have been minimized in the production of the recombinant spider silk referred to as 4RepCT (also further down denoted as wt), by reducing the number of repetitive sequences used for production (Fig. 2.1, right), along with other optimization procedures [7].

The number of repetitive sequences has been reduced in the recombinant silk protein 4RepCT, without losing the silk's ability to self-assemble into strong and elastic fibers [10]. As mentioned earlier, the 4RepCT recombinant spider silk can be expressed in a cloning host fused to another protein for functionalization [7, 8]. When functionalizing 4RepCT with antimicrobial peptides, the expressed fusion proteins maintain the silk's natural ability to self-assemble into silk fibers that could be used for biomaterials [8]. Hopefully, the biomaterial would also gain the bactericidal activity from the antimicrobial peptide. This would reduce the necessity of using conventional antibiotics when implanting a biomaterial, as the implant surface could be coated with the functionalized recombinant silk.

The possibility of using recombinant spider silk as a biomaterial is dependent on its biocompability. It would pose a problem to the possible applications of the recombinant silk biomaterial if the human body could not tolerate it. Initial studies have shown promising results for biocompability of the 4RepCT recombinant spider silk protein without functionalization [7, 15, 16]. Of course, functionalization of the spider silk protein with an antimicrobial peptide could influence the biocompability of the resulting material, which would need to be thoroughly tested before using it as a biomaterial *in vivo*.

2.2 Antimicrobial peptides

Antimicrobial peptides (AMPs) are small peptides with an antimicrobial effect, that are part of the innate immune response in many life forms. Depending on structure, size, charge and amino acid composition, AMPs are divided into groups and subgroups. Com-

mon for all AMPs, regardless of production organism, is that they are small, generally between 20-50 amino acids, and amphiphilic [17]. An important difference between bacteriocins, which are AMPs derived from bacteria, and antimicrobial peptides produced by eukaryotes, are the concentrations at which they are effective. Bacteriocins can be active at pico- or nano molar concentrations, while micro molar concentrations are often required for eukaryotic AMPs to be effective [18]. Eukaryotic AMPs are on the other hand often more broad spectrum, targeting many different microorganisms, while bacteriocins tend to have a narrow range, targeting a few species or a family of bacteria, often closely related to themselves [17, 18].

2.2.1 Target mechanism and antimicrobial activity

The exact target mechanism differ between AMPs and there are evidence suggesting that they affect bacteria in a multitude of ways [19, 20]. A key mechanism among most known AMPs seem to be a general targeting of microorganism's cell membrane, causing pores in the membrane (Fig.2.2). This can cause mortality by leakage of cell content, but the lethal effect of AMPs binding to microorganisms membrane also include inhibition of cell wall synthesis, nucleic acid and protein synthesis, enzyme activity and alternation of cytoplasmic membrane septum formation [19]. The general targeting ability of AMPs towards microorganism's cell membranes is one reason why using AMPs instead of conventional antibiotics could be advantageous. Conventional antibiotics often have a specific target site or process in the bacteria, that could render them ineffective if their target mechanism changes due to mutations in the bacteria. The general mechanism of AMPs, which often involves attractive forces between the peptide and the bacterial cell membrane is likely harder for bacteria to develop resistance against. Although, some resistance mechanisms towards antimicrobial peptides have been identified [21–24].

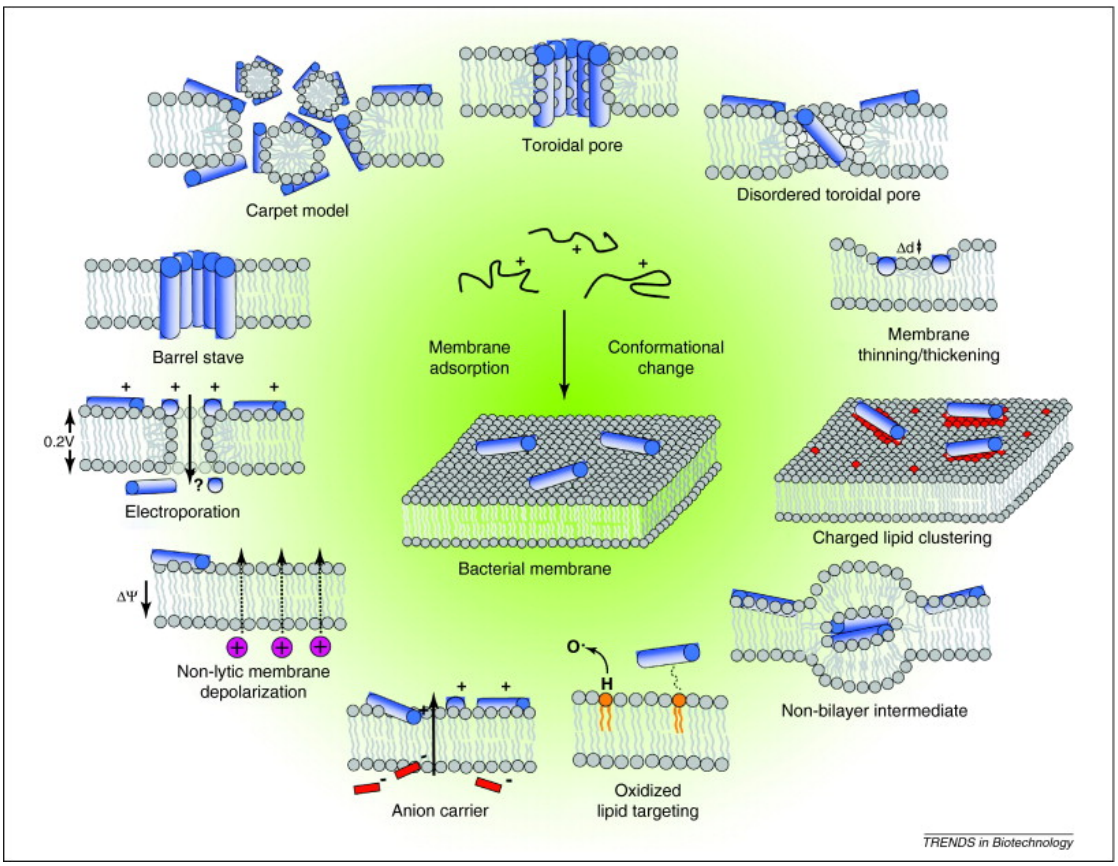

Figure 2.2: Suggested modes of action for antimicrobial peptide activity that could be initialized after antimicrobial peptide absorption to the bacterial cytoplasmic membrane. A threshold concentration of AMPs need to be reached to initialize membrane disturbance due to micelle formation in the carpet model, or pore formation from either the peptides in the barrel-stave model, or from peptides and lipids in the toroidal pore model. In the disordered torodial pore model, the pore formation involves fewer peptides and is more stochastic. The membrane thickness or configuration can also be effected by the peptides, or the peptides can induce non-bilayer intermediates. Other effects of the AMPs could be a targeting of oxidized phospholipids on the membrane or peptides coupling with small anions across the bilayer. The peptides could also influence the membrane potential, either with a non-lytic effect or with an increase of membrane permeability. The AMPs absorption to the bacterial membrane could induce one or many of these events. [20]

2.2.2 Using antimicrobial peptides for medical applications

The diversity in structure and functionality among antimicrobial peptides opens up for great possibilities to take advantage of their antimicrobial abilities, which is not limited to being only bactericidal. Among the more than 2500 AMPs known, some also have an effect against fungi, yeast, viruses and even tumors [19, 25]. There are however a few aspects to consider when utilizing AMPs for medical applications, besides the possible development of resistance towards them in bacteria. AMPs have been found to have an important role in regulating the microbiota and maintaining homeostasis in human intestine and skin, and both over- and under expression of AMPs in humans have been linked to disease [25]. Their specificity and durability are also factors to consider when developing applications using AMPs. Luckily, since AMPs are just short strings of amino acids, possible modifications can easily be achieved, which could help overcome these issues.

The AMPs chosen in this study needed to be functional in an immobilized state, as they were used to form a biomaterial in fusion with the spider silk protein. The material could be used for coating of implants or for other medical applications, where an antimicrobial effect is desired. During surgery and in a medical environment, patients are at high risk for exposure to infectious bacteria. The chosen AMPs have either previously shown promising results as to maintaining functionality in an immobilized state [26, 27], could be produced using the desired expression host [28], or their composition suggests a high efficiency against infectious bacteria [29].

Magainin I

Magainin I (Mag) is an 23 amino acid long antimicrobial peptide originally isolated from the African clawed frog *Xenopus laevis* [30]. The peptide is cationic and amphiphilic, containing both hydrophilic and hydrophobic residues [31]. A schematic representation of the primary and secondary structures can be found in Figure 2.3. The suggested mode of action for Magainin I is a disruption of cellular membranes by insertion of hyrophobic residues, pore formation and removal of membrane sections [32]. Magainin I has shown an antimicrobial effect against Gram positive bacteria when grafted on polymer brushes [33], and immobilized on gold surfaces [26]. Some strains of the Gram negative *Escherichia coli* have shown resistance development toward cationic AMPs such as Magainins, by alternating energy and nitrogen metabolism, amino acid conversion, stress response and cell wall thickness [24].

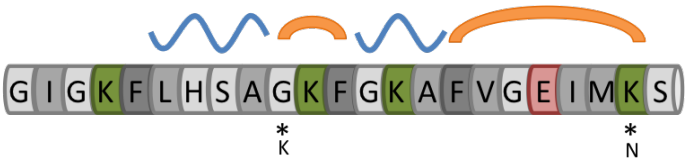

Figure 2.3: A schematic representation of Magainin I [8], where green indicates positively charged amino acids, red negatively charged and light and dark grey represents uncharged polar and non-polar amino acids respectively. The predicted secondary structure is represented with blue helixes and orange turns. The secondary structure is predicted for Magainin II, which differs in position 10 (Lys instead of Gly) and 22 (Asn instead of Lys) from Magainin I. The secondary structure was rendered from PDB-ID: 2LSA

A study that evaluated the use of modified cotton with immobilized Magainin I for wound dressing could see an inhibitory effect of the functionalized cotton on the Gram negative *Klebsiella pneumoniae* and Gram positive *Staphylococcus aureus* [27]. The same study also concluded no cytotoxic effects of Magainin I on human fibroblasts, rendering the AMP safe to use on human skin [27].

Lactoferricin

Lactoferricin (Lac) is a small antimicrobial peptide with a high density of positive charges. Out of its total 14 amino acids, 6 are cationic (Fig. 2.4). Lactoferricin is derived from the protein Lactoferrin, which is an iron-binding glycoprotein that can be found in milk from various mammals [34]. Lactoferricin has shown a broad activity against bacteria, virus, fungi and tumors [35]. However, a study of antibacterial activity of Lactoferricin immobilized to poly-hydroxyethylmethacrylate showed no antimicrobial effect against *Pseudomonas aeruginosa* and *Staphylococcus aureus*, suggesting that Lac might not be effective in an immobilized form [36]. However, immobilization to the surface is crucial when using the AMP fused to the spider silk protein as a coating material. Hopefully, the Lac-spider silk fusion protein could show an antimicrobial effect in an immobilized form even if the Lac peptide on its own might not.

Figure 2.4: A schematic representation of Lactoferricin [8], where green indicates positively charged amino acids and light and dark grey represents uncharged polar and non-polar amino acids respectively. The arrow represents a beta sheet in the predicted secondary structure, along with an orange turn. The secondary structure was rendered from PDB-ID: 1LFC

WGR

The GRR10W4 (herein referred to as WGR) is a short, hydrophilic and highly charged peptide consising of 14 amino acids (Fig. 2.5) [37]. Unlike Magainin I and Lactoferricin, which are naturally occuring AMPs, the WGR peptide is a synthetically constructed AMP derived from the human proline arginine-rich and leucine-rich repeat protein (PRELP) [37]. Schmidtchen et. al [37] found that end-tagging antimicrobial peptides with oligotryptophan promotes peptide-induced lysis of phospholipid liposomes, as well as membrane rupture and killing of bacteria and fungi.

Figure 2.5: A schematic representation of the antimicrobial peptide referred to as WGR, where green indicates positively charged amino acids and light and dark grey represents uncharged polar and non-polar amino acids respectively. The peptide is synthetically constructed and not present in the protein database (pdb.org). Mainly random coil was predicted using the secondary structure prediction tool GOR IV.

2.3 Infectious bacteria

Infectious bacteria are bacteria that enters the body and produces toxins, which causes illness. The same bacteria that are mostly harmless or even helpful, might be pathogenic under certain conditions. The gram positive *Staphylococcus aureus*, commonly present on our skin, or the gram negative *Pseudomonas aeruginosa* and *Escherichia coli*, are so called opportunistic pathogens. That means that they are normally kept under control by the immune system, but can cause infections when the immune system is deprived or if they enter the body where they are normally not present.

2.3.1 Biofilm formation

Some bacteria have the ability to form a biofilm, which consists of bacterial cells sticking together in a network, often adhered to a surface. The formation typically starts with a few bacteria adhering to a surface through hydrophobic interaction or van der Waals forces. The adhesion could be reversible, or the bacteria could get a tighter grip by attaching cell structures for adhesion, such as fili, on the surface. Once adhesion has begun, the biofilm can start growing through bacteria division and recruitment. As the biofilm grows, bacteria start to form an extracellular matrix of molecules that protects the biofilm, enhances signaling and helps distribution of nutrients. Typically, the extracellular matrix consist of polysaccharides. Eventually, the biofilm is mature enough to disperse bacteria into the surrounding, which can then start to colonize elsewhere.

Biofilms work as protection for the bacteria within, where only the surface of the biofilm is exposed to the surrounding environment. This is especially problematic when trying to battle infections caused by biofilm forming bacteria, as antibiotics may not be able to penetrate the biofilm. The resistance to antibiotics after biofilm formation can increase a thousandfold compared to free floating bacteria of the same species [38].

2.3.2 Commonly encountered infectious bacteria

The application for the AMP-silk fusion proteins used in this study is as a biomaterial, where the antimicrobial peptides are meant to work as an substitute to conventional antibiotics. As such, the preferable antimicrobial effect should be against bacteria commonly causing infections in a hospital environment.

Pseudomonas aeruginosa is one species of bacteria that are currently posing problems due to resistance development to a wide variety of antibiotics [39]. The Gram negative bacteria *Escherichia coli* and the Gram positive bacteria *Staphylococcus aureus* are often involved in biofilm formation on implants [5]. The effect of the AMP-silk fusion proteins on these bacteria are therefore of interest, since one possible application for the fusion proteins could be as a coating on implants.

2.4 Confocal laser scanning microscopy

Confocal laser scanning microscopy (CLSM) can be used to visualize bacteria in high resolution with the help of lasers and fluorescent dyes. Optical sectioning is utilized in the microscope, which means that the projected image is obtained from only a small section at a chosen depth in the sample, eliminating the need to sectioning the sample beforehand. As the sample is illuminated one depth level, or focal plane, at the time, the background noise that would be present if using a regular fluorescent microscope is almost eliminated using the CSLM. The depth of focus is chosen by the operator, so the thickness of a bacteria film could easily be measured using this microscopy technique.

The confocal laser scanning microscope uses a laser beam that is passed through an aperture, which is a small pinhole that controls the light flow (Fig. 2.6). The light passes through an objective lens, which focuses the beam onto the focal plane of the investigated specimen. Light from the illuminated sample, along with reflected light from the laser, travels back through the objective lens and passes through a dichroic mirror, that filters out light at the original wavelength and let light at specific wavelengths pass through to a detector. The detector transforms the light signal into an electric signal that can be interpreted by a computer as an image of the specimen.

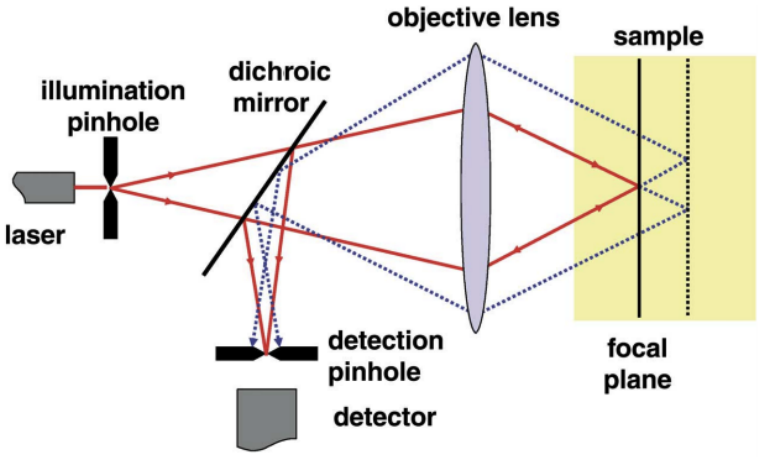

Figure 2.6: The principle of confocal laser scanning microscopy. Light at a specific wavelength enters the illumination hole which controls the light flow. The light passes through an objective lens and is focused onto a specific depth of the studied sample, the focal plane. Emitted light from the sample and reflected light from the laser passes back through a dichronic mirror, which filters out the original wavelength and passes on light from set wavelengths. Light of correct wavelengths is passed through a detection pinhole into a detector that can transfer the signal to a computer. [40]

3

Materials and Methods

The recombinant silk proteins, containing either of the three antimicrobial peptides, have previously been transformed to *Escherichia coli* strain NovaBlue (Merck Millipore) and amplified in *E. coli* BL21(DE3) (Merck Biosciences) [8]. The cultures were stored in freezer (-80°C) as 15% glycerol stocks before use for protein purification.

3.1 Protein production and purification

Expression of proteins from the transformed cultures was started by thawing cells from the glycerol stocks and inoculate in LB-medium with kanamycin (70 μg/mL final concentration). The cultures were incubated for 30 minutes (30°C, 180 rpm) before the rotation was increased to 220 rpm. Cells were further incubated until an OD_{600} of 0.8-1.0 was reached. The incubated cultures were cooled to 15°C before protein expression was induced by adding isopropyl β-D-thiogalactosidase (IPTG) (0.3 mM final concentration), followed by culturing for 18 hours. Cells were harvested by centrifuging (20 min, 5000 rpm, 4°C) and the harvested pellet was dissolved in Tris(hydroxymethyl)aminomethane (20 mM, pH 8) and kept frozen (-20°C) until protein purification. The fusion proteins containing Mag and Lac respectively, were previously purified and stored in freezer (-20°C) until use for preparation of the testing material [8]. 4RepCT silk protein used as reference (herein denoted wt for wild type), was kindly provided by Spiber Technologies AB.

3.1.1 Purification of WGR-silk fusion protein

Harvested cells that had expressed the WGR-silk fusion protein were thawed in cold water during which CHAPS detergent, Complete and Pepsatin A were added and left to incubate for 30 minutes. Lysing of cells was performed by adding lysozyme-A, DNAseI and $MgCl_2$ before incubation for 1 hour. NaCl was added to the lysed cells (200 mM final concentration) before centrifuging (30 min, 10000 rpm, 4°C) and the supernatant, containing soluble proteins, was filtered. The filtered protein solution was added to a HisTrap column (HP, 1 mL), equilibrated in 20 mM Tris and 200 mM NaCl and purified using ÄKTA^{TM} Explorer system. The column was washed with 20 mM Tris, 200 mM NaCl and increasing amounts of Imidazole (500 mM) to eluate the target protein. His-tags and thioredoxin at the N-terminus of the target protein were cleaved off by adding Protease 3C (100 µg/mg target protein) and dithiothreitol to the eluate before dialyzation overnight (20 mM tris, 200 mM NaCl, 4°C, 6-8000 MWCO). The cleaved target protein was centrifuged (4000 g, 10 min, 4°C) before the supernatant was added to Ni-NTA-agarose columns to separate it from the cleaved off His-tags, thioredoxin and Protease 3C residues. The flow through was collected and concentrated using Amicon Ultra Centrifugal Filter Units, 3000 MWCO. The result from the protein purification was verified by reducing conditions sodium dodecyl sulfate polyacrylamide gel electrophoresis (SDS-PAGE).

3.1.2 Evaluation of purified WGR-silk fusion protein functionality

An evaluation of the functionality of the WGR-silk fusion protein was done by creating fibers from the purified protein. The procedure was performed using previously developed methods for fiber formation [7]. Formed fibers were photographed using a light microscope.

3.2 Preparation of disks for antimicrobial activity assays

Polystyrene disks (Θ 0,8 cm) were coated either with a AMP-silk fusion protein, or recombinant spider silk without functionalization (wt). Films of the silk material was formed on the disks by incubating them with 0.05 mg of the purified silk protein solution

in Tris (20 mM) for 30 minutes. The coated disks were washed twice with Tris (20 mM), and stored in room temperature under sterile conditions until use. Uncoated disks, used as a negative reference, were incubated with Tris (20Mm) for 30 minutes before washing.

3.3 Antimicrobial activity assays

To evaluate the antimicrobial effect of the AMP-silk fusion proteins, coated disks were transferred into sterile flasks and inoculated with overnight cultures of *Escherichia coli*, *Pseudomonas aeruginosa* or *Staphylococcus aureus*. Depending on evaluation method, disks were incubated with diluted overnight bacterial cultures for different durations, either 5, 24 or 48 hours. The two methods used to evaluate bacteria viability after incubation was to determine the number of colony forming units (CFU) adhered to the disks and to examine the disk's surfaces using confocal laser scanning microscopy.

3.3.1 Strains and overnight cultures

For both evaluation methods, overnight cultures of *Escherichia coli* TG1 [41], *Pseudomonas aeruginosa* PA14 [42] and *Staphylococcus aureus* SH1000 [43] were used. The cultures were prepared from colonies of each bacterial strain, grown on Tryptic Soy Agar (TSA) plates (re-streaked weekly), by inoculating a few colonies from the plates in 10 ml Tryptic Soy Broth (TSB) and incubate overnight (19-20 h, 37°C). The liquid cultures were diluted 10 000 times in TSB to a final concentration of approximately $5*10^4$ CFU/ml, which was previously determined by CFU trials.

3.3.2 Colony forming units

Colony forming units are determined by adding a small volume of bacterial culture in dilution series to agar plates that are incubated overnight. Each viable bacteria is able to start a new colony which, after incubation, is large enough to be visible for counting. The number of formed colonies on the plate is multiplied with the dilution factor, to determine the total number of colony forming units per volume in the original sample.

Determination of CFU of bacteria adhered to the disk's surfaces was done after incubation (5 h, 37°C) with 1 ml from the diluted overnight bacterial cultures. Disks were washed by gently dipping them in 2 ml peptone water and removing excess fluid with a lens paper, before transferring them to new vials with 1 ml peptone water. Vials were vortexed (1 min), sonicated (35 kHz, 10 mins) and vortexed again (1 min) to detach adherent bacteria from the disks. Dilutions were made of the vial content and duplicates of the dilutions were spread on TSA plates in aliquots of 20 µL. Dilutions of the growth medium were also made and spread to determine the number of CFU in the medium after incubation. Plates were incubated (17 h, 37°C) and colonies were counted.

Evaluation of sonication and vortexing effect on bacteria

The bacteria viability before and after the sonication and vortexing procedure was determined using a similar set up as for the CFU trials. The same growth conditions applied, but instead of incubation on disks, bacteria from the overnight cultures were incubated for 5 hours in vials without any disks. Bacteria from the incubated vial was diluted 100 times in peptone water in a new vial, to roughly simulate the same growth conditions as the bacteria adhered to disks would have after transferring to new vials before the vortexing and sonication procedure. Streak outs for CFU was done before and after the vials were vortexed and sonicated, to determine the effect on bacteria viability of the vortex and sonication procedure used in the trials.

3.3.3 Confocal laser scanning microscopy

For determination of bacteria viability using CLSM, the bacteria first needed to be stained for visualization. This was done using the LIVE/DEAD® BacLight™ Bacterial Viability kit, where bacteria were stained with CYTO 9 and propidium iodide. CYTO 9 is a membrane permeable dye that stains nucleic acid in both live and dead bacteria, while propidium iodide can only enter cells with a disrupted cell membrane. Therefore, all bacteria would be stained by CYTO 9, but only bacteria with disrupted cell membranes, i.e. dead bacteria, become stained by propidium iodide. The two stains get excited by light of different wavelengths and upon excitation emit light at a range of wavelengths that can be detected and translated as green light from live cells and red light from dead cells.

Investigation of bacterial coverage on disks

Disks were incubated (24 h or 48 h, 37°C) with 1 mL of the diluted overnight cultures of either of the three bacterial species in TSB. Dye stock solution for LIVE/DEAD®-staining was prepared by mixing peptone water, CYTO 9 and propidium iodide in a 8:1:1 ratio. The incubated disks were washed by gently dipping them in 2 ml peptone water and removing excess fluid against a lens paper, before staining them with 15 µL dye stock solution. The disks were examined directly after staining using CLSM (Leica TCS SP2, Heidelberg, Germany). The object used for examination was a water immersion HCXPL APO with 63x magnification and 1.20 numerical apeture. The light sources were Ne/He and Ar lasers set to λ_{ex}=594 nm (propidium iodide) and λ_{ex}=488 nm (CYTO 9) respectively. Emission signals were captured at wavelengths between 510-540 nm for CYTO 9 (green/live cells) and 620-650 nm for propidium iodine (red/dead cells). 20-30 digital images were captured of every disk (400 Hz scanning frequency, 8 line average, 1024x1024 resolution) and analyzed using MATLAB, with a software developed at SP Food and Bioscience, Sweden. The software calculated the area fractions of live and dead cells in a thin optical section close to the disk surface.

Biofilm thickness measurement

The thickness of the bacterial biofilms attached to the surfaces of the disks was measured at approximately 10 places on each disk, taking two different measurements at each location. One measurement was taken at the thickness of the main layer of biofilm at that place, and one measurement was taken at the thickest part of the biofilm at that place (Fig. 3.1). Sometimes, the thickest part and the main layer would be the same thickness, if the layer of biofilm was even. In those cases, no measurement was taken for the thickest part. However, at most places, clusters were formed by the bacteria, which stretched out from the main layer. The measurements were taken using CLSM, by starting at the disk surface as a reference point and move the focal plane in z-direction until the thickness of the main layer and thickest part of the biofilm was reached, noting the movement in z-direction.

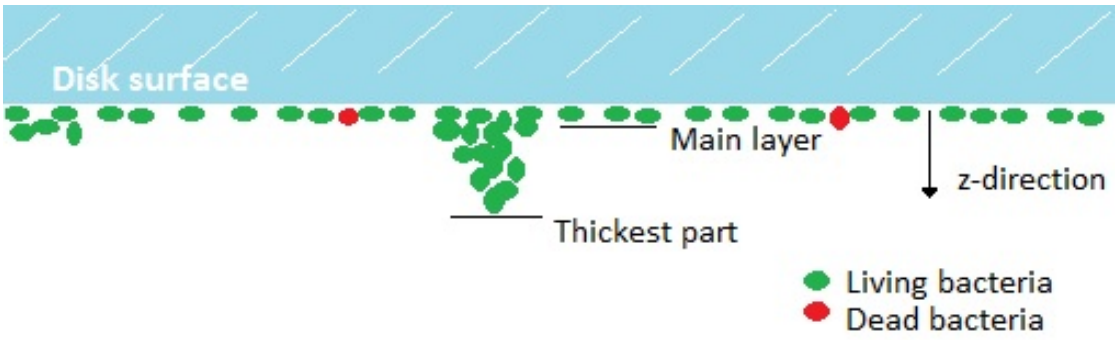

Figure 3.1: A schematic representation of the bacterial biofilm layer formed on the disk's surface, where green and red ovals represent live and dead bacteria. Lines indicate where the thickness measurements for the main layer and thickest part of the biofilms were taken.

3.4 Statistical analysis

The results from the antimicrobial activity assays were tested for statistical significance in MatLab using one-way analysis of variance (ANOVA) to determine if the sample means of each treatment (wt, antimicrobial peptides and uncoated) significantly differed from each other. Multiple comparison between treatments was performed by applying Tukey's range test to the ANOVA results, to establish between which treatments any significant differences occurred. Individual unpaired t-tests were also performed in some cases, to show trends in the results. This was done because the ANOVA and following post hoc investigation conducted using Tukey's range test is more strict than individual t-tests. The ANOVA and multiple comparison approch is a better way than individual t-testing when investigating several treatment groups, since the risk of performing a type-I error (an incorrect rejection of a true null-hypothesis) increases when conducting multiple individual t-tests. Individual t-testing could sometimes still be useful to show trends in the results that might not be significant in the ANOVA- and multiple comparison analysis.

The critical p-value to reject the null hypothesis (no significant difference between treatment means) was set to 0.05, where a lower p-value indicates a significant difference between treatments. A p-value of 0.05 is equal to a 95% confidence interval, which denotes the probability that any significant differences between treatments were due to the different coatings, and not due to random errors.

4

Results

This section presents results from the protein purification and functionality investigation of the WGR-silk fusion protein. The section also includes the results from the antimicrobial activity assays conducted of the wildtype (wt) spider silk protein and the Lactoferricin-, Magainin I- and WGR-silk fusion proteins on *Escherichia coli Pseudomonas aeruginosa* and *Staphylococcus aureus*.

4.1 Purification and function of WGR-silk fusion protein

An SDS-PAGE gel displays the result from the purification of WGR-silk fusion protein (Fig. 4.1). The marked band correspond to the theoretical molecular weight of the WGR-silk fusion protein before (40,4 kDa) (Fig. 4.1, well 2) and after (25.7 kDa) (Fig. 4.1, wells 4 and 5) cleavage from the thioredoxin and his-tag with Protease 3C. The purified WGR-silk fusion protein showed ability to form silk fibers (Fig. 4.2).

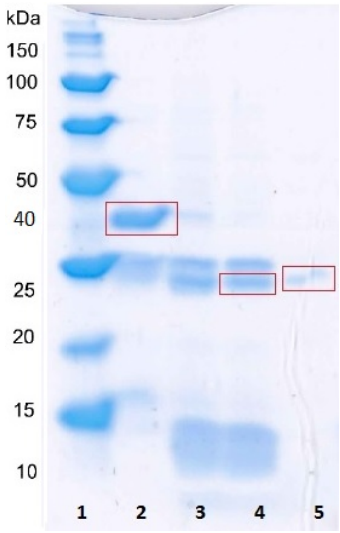

Figure 4.1: SDS-PAGE analysis of purified WGR-silk fusion protein. Wells were loaded with: 1. Low molecular weight ladder. 2. Uncleaved target protein from ÄKTA-purification with added 3C Protease. 3. Pellet from centrifugation with cleaved target protein. 4. Supernatant from centrifugation with cleaved target protein. 5. Supernatant after flow through Ni-NTA-agarose column. Marked bands corresponds to the theoretical molecular weight of the WGR-silk fusion protein before (40.4 kDa) and after (25.7 kDa) cleavage from the thioredoxin and His-tag. The band in well 5 is slightly distorted due to a rupture in the gel.

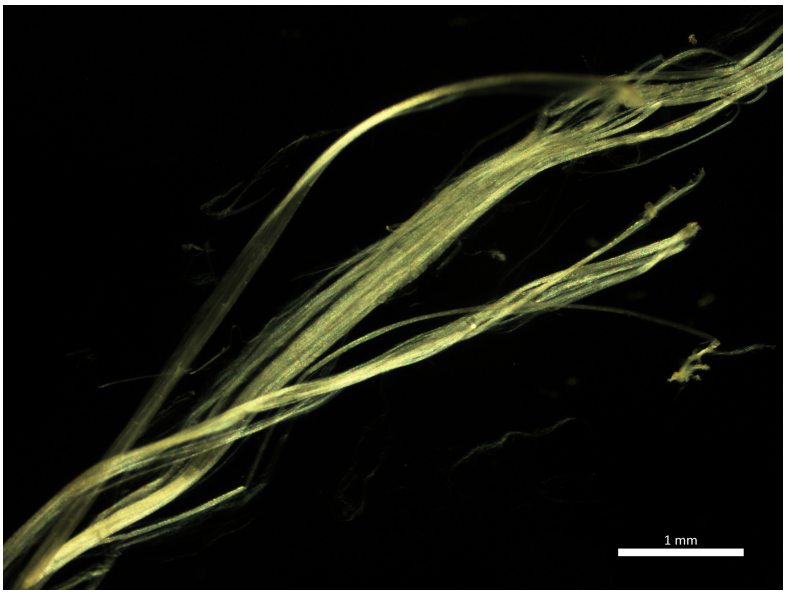

Figure 4.2: Fiber formed of purified WGR-silk fusion protein, photographed using a light microscope with 2x magnification.

4.2 Antimicrobial activity assays

Results from the colony forming unit investigations and the confocal laser scanning microscopy of bacterial growth on the disks are only presented for *E.coli* and *S. aureus*. The CLSM- and CFU-investigations of *P. aeruginosa* showed no bacteria adhered to the disk's surfaces of wild type and uncoated disks, and a low CFU count. Further investigations were not performed on the *P. aeruginosa* bacterial species.

4.2.1 Colony forming units

Results from the CFU-count of detached bacteria from wt, Lac, Mag, WGR and uncoated disks, after 5 hours of incubation with *E. coli* and *S. aureus*, are displayed in Figure 4.3. The CFU-count was conducted on triplicates of each type of disk and revealed a high variance between the replicates, especially for *S. aureus*. No significant differences between disks were found for either of the bacteria species using ANOVA-analysis. However, significantly less CFU/ml were present after the sonication detachment procedure on Mag-silk disks incubated with *E. coli* than on wt disks, when performing a single t-test on these CFU counts (p=0.0047) (Fig. 4.3).

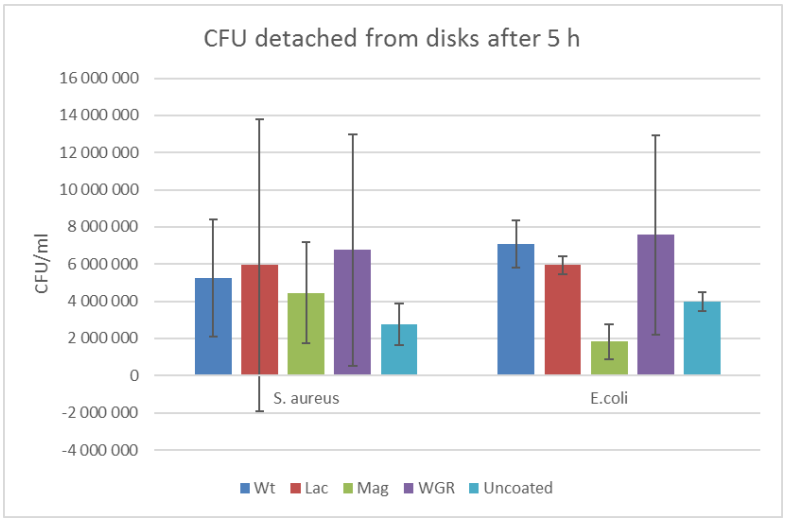

Figure 4.3: Colony forming units (CFU/ml) detached from wt, AMP-silk fusion proteins or uncoated disks, after 5 hours of incubation with overnight cultures of *S. aureus* and *E. coli*. Bars are based on mean values of triplicates with error bars displaying standard deviations.

No significant differences between disks were detected for number of CFU/ml in the incubation medium after cultivation for 5 hours with *E. coli* or *S. aureus* (Fig. 4.4a). A significant increase of bacterial CFU/ml for both species (p=0.0092 for *S. aureus* and p=0.0395 for *E. coli*, using paired t-tests) occurred after the performed vortexing and sonication procedure, which was used to detach bacteria from the disks in the CFU-trials (Fig. 4.4b).

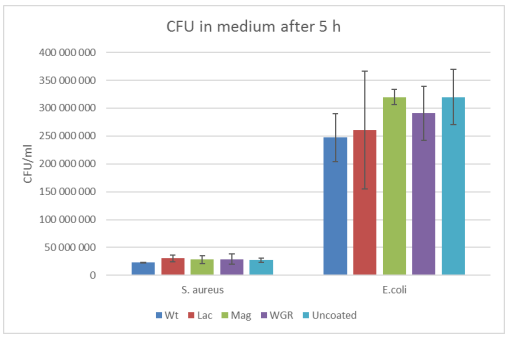

(a) CFU in medium after 5 h of incubation

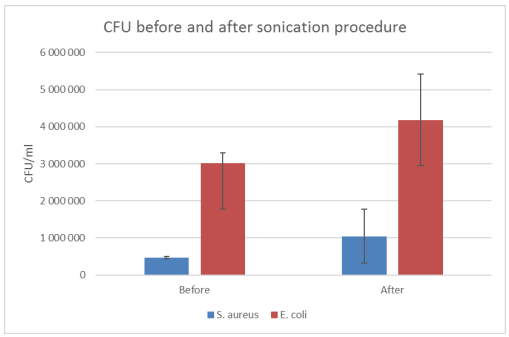

(b) CFU before and after vortexing and sonication procedure

Figure 4.4: Subfigure (a) displays colony forming units (CFU/ml) in the medium after 5 hours of incubation with overnight cultures of *S. aureus* and *E. coli* on wt, AMP-silk fusion proteins or uncoated disks. Subfigure (b) displays the effect of the vortexing+sonication+vortexing procedure on the colony forming units (CFU/ml) after 5 hours of incubation with the overnight cultures without disks. Bars are based on mean values of triplicates with error bars displaying standard deviations.

4.2.2 Confocal laser scanning microscopy

Results from the investigation of bacterial growth on disks using CLSM are presented for the living fraction of bacteria that covered the disks (Fig. 4.5–4.8). The amount of dead bacteria on the disk's surfaces was very low in comparison. Results from the thickness measurements of the biofilm formed by *E. coli* after 24 hours of incubation (Fig. 4.6) and *S. aureus* after 24 and 48 hours (Fig. 4.9) of incubation on the disks are also presented.

Antimicrobial assays with *Escherichia coli*

ANOVA-analysis was performed on five replicates of WGR, four replicates of wt and Lac, and triplicates of Mag and uncoated disks (Fig. 4.5). No significant differences were found between fractions of disks covered with living *E. coli* after 24 hours of incubation (Fig. 4.5). However, single t-tests revealed significantly less bacterial coverage on wt disks compared to uncoated (p=0.0318) and between Mag-silk and uncoated (p=0.0172) disks.

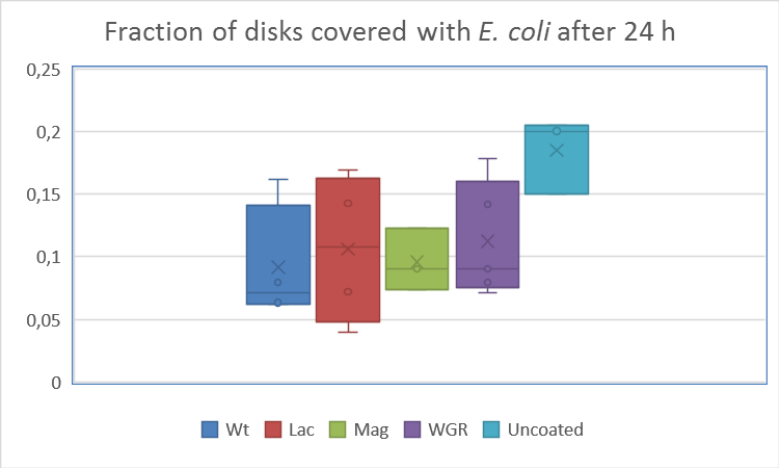

Figure 4.5: Fraction of wt, AMP-silk fusion protein coatings and uncoated disks covered with living *E. coli* after 24 hours. Boxes extend from the 25:th to the 75:th percentiles and the whiskers extend to the most extreme data points. The lines inside the boxes represents medians, the crosses represents mean values and the circles represent data points.

Biofilm thickness analysis (Fig. 4.6) were performed on the same replicates that were included in the bacterial coverage investigation (Fig. 4.5). No significant differences were found between disks' thickness of biofilm formed by *E. coli* after 24 hours (Fig. 4.6), using ANOVA-analysis. Single t-tests however, revealed a significantly thinner *E. coli* biofilm at the thickest place of Lac disks compared to uncoated disks (p=0.0446), and on Mag-silk disks compared to uncoated disks (p=0.0461), after 24 hours of incubation (Fig.4.6). A single t-test also showed a significantly thinner main layer of *E. coli* biofilm formed on wt disks compared to uncoated disks (p=0.0448) (Fig.4.6).

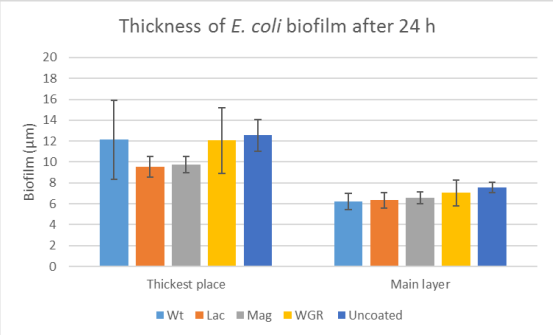

Figure 4.6: Thickness of *E. coli* biofilm (µm) after incubation for 24 hours on wt, AMP-silk fusion proteins or uncoated disks. Bars are based on mean values of measurements from three to five sample disks, with error bars displaying standard deviations.

Antimicrobial assays with *Staphylococcus aureus*

The fraction of disks covered with living *S. aureus* after 24 hours (Fig. 4.7) and 48 hours (Fig. 4.8) of incubation differed between disks, depending on disk's coating. Significantly less bacteria covered Mag-silk disks compared to uncoated (p=0.0141) and WGR-silk disks compared to uncoated (p=0.001) after 24 hours of incubation, according to ANOVA-analysis and Tukey's range test (Fig. 4.7). The analysis was performed on five replicates of wt, Mag and uncoated disks, and on four replicates of Lac and WGR.

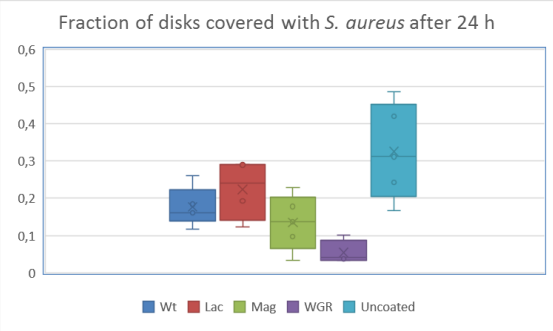

Figure 4.7: Fraction of wt, AMP-silk fusion protein coatings and uncoated disks covered with living *S. aureus* after 24 hours. Boxes extend from the 25:th to the 75:th percentiles and the whiskers extend to the most extreme data points. The lines inside the boxes represents medians, the crosses represents mean values and the circles represents data points.

The ANOVA-analysis and Tukey's range test of *S. aureus* coverage of disks after 48 hours of incubation showed a significantly lower amount of bacteria on all the coated disks compared to the uncoated ones (Fig. 4.8). Analysis was performed on six replicates of wt, five replicates of Mag and Lac, four replicates of uncoated disks and triplicates of WGR disks. The most significant difference in fraction of live bacteria covering the disks after 48 hours of incubation was between the Lac and uncoated disks (p=0.0002), followed by WGR- and uncoated (p=0.0004), Mag- and uncoated (p=0.0006) and wt and uncoated disks (p=0.0076) (4.8a).

Removing outliers (one disk each from wt, Lac and Mag, with values extending far outside of the 25:th and 75:th percentiles) also revealed significantly less bacterial coverage on disks coated with either of the AMP-silks compared to wt (Fig. 4.8b). The removal of the outliers introduced a significantly lower coverage of *S. aureus* on Lac compared to wt (p=0.0198), Mag compared to wt (p=0.0378) and WGR compared to wt (p=0.0389) disks, as well as strengthening the significance of the already observed differences between the coated and uncoated disks (Fig. 4.8b).

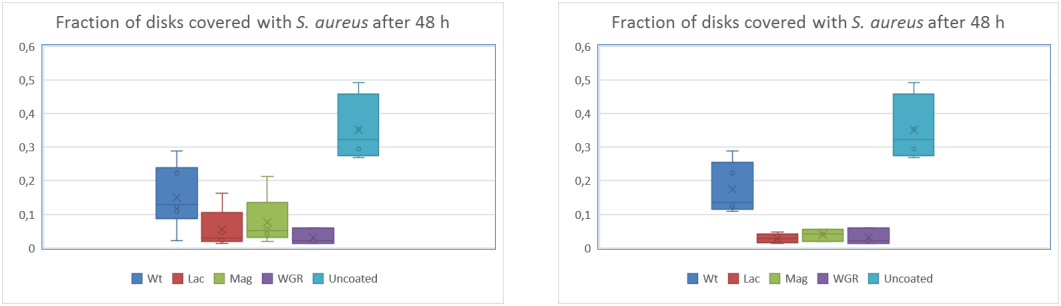

(a) Including outliers **(b)** Outliers removed

Figure 4.8: Fraction of wt, AMP-silk fusion protein coatings and uncoated disks covered with living *S. aureus* after 48 hours. Boxes extend from the 25:th to the 75:th percentiles and the whiskers extend to the most extreme data points. The lines inside the boxes represents medians, the crosses represents mean values and the circles represents each data point. In subfigure (a), data from all disks are included, while in subfigure (b), one disk each from wt, Lac and Mag, regarded as outliers (with values extending far outside of the 25:th and 75:th percentiles), has been excluded.

Analyses of *S. aureus* biofilm thickness after 24 and 48 hours of incubation (Fig. 4.9) on the coated disks were performed on the same replicates that were analyzed in the bacterial coverage investigations (with outliers excluded for the 48 h incubation). ANOVA-analysis of the biofilm thickness measurements from disks incubated with *S. aureus* for 24 hours showed a significant difference in variance between disks (p=0.0409 for the thickest place, p=0.0473 for the main layer). The multicomparison on the ANOVA-results

however, using Tukey's range test, did not reveal any significant differences between coatings. The difference in biofilm thickness on the WGR- and Mag disks compared to the uncoated disks came closes to a statistical significance using Tukey's range test on the ANOVA-results (p=0.060 for WGR compared to uncoated, thickest place and p=0.0522 between Mag and uncoated, main layer)(Fig. 4.9a). No significant differences between disks were found when performing ANOVA-analysis on the biofilm thickness measurements of *S. aureus* after 48 hours of incubation (Fig. 4.9b). However, all AMP-silks had significantly thinner main layer biofilms than uncoated disks, when analysis was performed using single t-tests (Fig. 4.9b).

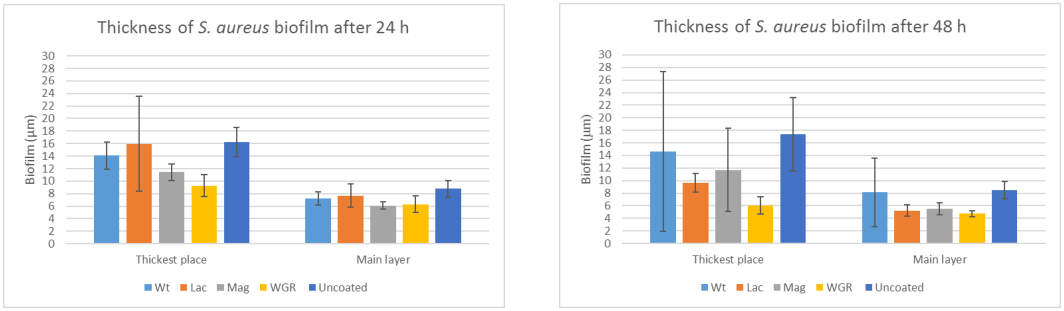

(a) *S. aureus* biofilm thickness after 24 hours. **(b)** *S. aureus* biofilm thickness after 48 hours.

Figure 4.9: Thickness of *S. aureus* biofilm (µm) after incubation for 24 hours (a) and 48 hours (b) on wt, AMP-silk fusion proteins or uncoated disks. Bars are based on mean values of measurements from three to five sample disks, with error bars displaying standard deviations.

5

Discussion

The results from the WGR-silk fusion protein purification and antimicrobial activity assays of the AMP-silk constructs are discussed in this section. The section includes suggestions on how to improve the methods used for purification of the constructs, along with assessments and discussions of the methods used to evaluate antimicrobial activity, and how the results were interpreted.

5.1 Purification efficiency of WGR-silk fusion protein

The results from the purification of WGR-silk fusion protein showed that the protein construct could be expressed using standard procedures in an *E. coli* host, which is beneficial if the protein production is going to be scaled up. It was possible to purify the WGR-silk protein construct using an ÄKTA^{TM} Explorer setup and HisTrap column, where the target protein was able to bind to the column through the his-tag on the construct and be eluted with Imidazol (Fig. 4.1). The yield of WGR-silk protein that can be purified from the total amount of expressed protein could be improved by modifying the previously described procedure. One indication that improvements can be made could be seen on the SDS-PAGE, where a band of the same theoretical weight as the target protein (25.7 kDa) seem to still be present in the pellet after centrifugation (Fig. 4.1, well 3). More target protein could likely be collected from this pellet by dissolving it again, possibly improving the solubility of the protein by using a different buffer composition. Other modifications that could improve the purification procedure include changing the concentrations and gradients of salt and Imidazol, the elution time, and the time for cleavage and dialysis to try to avoid protein aggregation during production, as aggregated protein is malfunctional.

Using a bacterial host to express AMP-protein constructs could seem illogical, seeing as the constructs are designed to kill bacteria. Bacterial growth seemed unaffected by the expressed AMP-silk proteins during cultivation. The AMP-part of the constructs were likely blocked from activity during expression in the host, with a His-tag and thiorodexin domain at the N-terminus, and the silk-protein at the C-terminus, surrounding the AMPs [8]. The tags were cleaved off during protein purification, making the AMPs free to interact with bacterial membranes again.

It is the silk part of the construct that can make coatings on materials, which should leave the AMP-part free to interact with it's environment. Depending on the thickness of the AMP-silk coating, silk-proteins could likely entrap AMPs inside the structure if the coating is thicker than one monolayer, which could hinder the AMPs from performing any activity on surrounding bacteria. Still, the top layer of the coating should have the AMP-part of the construct facing outward to the environment, enabling interaction with bacterial membranes.

The fact that the AMP-silk constructs were able to form fibers (Fig. 4.2) and films [8] showed maintained functionality of the silk even after functionalization with the AMPs. This suggests that the AMP-silks possess the same structural abilities as wt silk, which would enable a range of possible structures being formed with AMP-silks, including films, fibers, meshes and foams [7].

5.2 Evaluation of the antimicrobial activity assays

The antimicrobial activity assays were separated into two methods; counting the colony forming units formed on the coated disks and calculate the fraction of the disks covered by bacteria after cultivation. Included in the latter were also measurements of the bacterial biofilm thickness. Both methods were carried out using diluted overnight cultures of *E. coli*, *P. aeruginosa* and *S. aureus*. The experimental setup was from start proving to be difficult to use for evaluation of the antimicrobial effect of the AMP-silks on *P. aeuroginosa*.

5.2.1 Evaluation methods not suitable for *P. aeruginosa*

After cultivation of *P. aeruginosa* on duplicates of wild type disks, the LIVE/DEAD staining and CLSM showed no adhered bacteria on the disk surfaces. Bacteria were present in the samples, but only on the microscope cover glass. These bacteria confirmed that there had been bacteria growing in the incubation medium, but they had not adhered to the surface of the disks. Bacteria on the cover glass were not relevant for analysis, since the comparison between disks were performed on bacteria that had been in contact with the disk's surfaces and adhered to the disks. As these disk were to be used as reference for antimicrobial activity evaluation of the AMP-silk fusion proteins, and they did not contain any bacteria, the analysis of the antimicrobial effect of the AMPs on this bacteria strain could not be conducted using this method.

To evaluate if the lack of *P. aeruginosa* adhered to the wt disks could have been due to an antimicrobial effect of the spider protein itself, an uncoated disk was incubated under the same conditions as the wt disks. The uncoated disk showed the same result as the wt disks, bacteria were present in the medium, but did not adhere to the disk surface. Therefore, it was concluded that *P. aeruginosa* either did not form a biofilm on the polystyrene material under the used growth conditions, or it was too easily washed away before analysis.

The first set of CFU trials that was performed on *P. aeruginosa* showed a much lower CFU count after detachment from the disks than the other two bacterial species, which confirmed that the bacteria did not adhere to the disks. No further trials were therefore made on *P. aeruginosa*.

5.2.2 Large variation between replicates in CFU-trials

Large variations occurred between replicates in the CFU-trials (Fig. 4.3 and 4.4a). This was problematic when evaluating the results from these trials, since possible differences between the AMP-silks, wt and uncoated disks would be hard to establish, without performing a large number of replicates of the trials. Unfortunately, triplicates of each type of disk incubated with *E. coli* or *S. aureus* did not generate enough data to establish any significant differences between treatments. More replicates could have established significant differences between the coatings, since t-tests of the results already indicated a lower CFU count on Mag compared to wt for disks incubated with *E. coli*.

The large variation between replicates could also indicate that the investigation method was too sensitive to differences in the experimental setup between trials. If small differences in the conditions during the experiment introduced the large variations, the method might not have been a good way to test the antimicrobial activity of the AMP-silks.

5.2.3 Sonication procedure had a positive effect on bacteria viability

The sonication and vortexing procedure that was used to detach bacteria from the disks during the CFU-trials was assumed not to effect bacteria viability, but the CFU count increased significantly after the procedure (Fig. 4.4b). This could have been due partly to the time difference between the streak-outs that were made on TSA-plates before and after the sonication and vortexing procedure. Since bacteria dilutions were made in peptone water, a medium that would not halter continuous growth of the bacteria, the time difference between streak-outs would affect the number of CFUs on the plates, if bacteria kept on growing in the solution. This could have been avoided by using a dilution medium that would prevent growth, but still maintain bacteria viability.

Another possible explanation to the higher CFU count after the sonication and vortexing procedure could be that the sonication might have separated bacteria from each other, so that two conjoined bacteria that would have formed one colony before the sonication, afterwards would form two separate colonies instead.

5.2.4 Alternative method for CFU-trials

An alternative method to the conducted CFU-counts, that might have generated less variation between replicates, could have been to dilute the overnight cultures much more, so that they only contained a few bacteria. A small volume of the diluted cultures could have been incubated on the AMP-silk disks and enclosed in TSA, to see if the few bacteria on the disks were able to form any colonies, or if the AMP-silks would inhibit colony formation.

5.2.5 AMP-silks' efficiency differed between species of bacteria

The investigation of bacterial coverage of disks had less variation between replicates than the CFU-trials. Results from the analyses of the pictures taken of each disk showed a significantly lower amount of live bacteria on all the AMP-silk disks incubated with *S. aureus* than the wt and uncoated disks after 48 hours, when outlier disks were removed from the analysis (Fig. 4.8b). A decrease of bacterial adhesion, thought to be due to an antimicrobial effect of the Mag- and WGR-silks, could be seen already after 24 hours on this bacterial species (Fig. 4.7). The AMP-silks were not as effective on the Gram negative *E. coli* (Fig. 4.5), where a significant decrease in bacteria adhesion could only be seen on the wt and Mag disks compared to uncoated disks. This antimicrobial effect could have been contributed by the silk itself, without addition of the AMP, since there was no significant difference between the wt and Mag disks. The differences in antimicrobial effect of the AMP-silks on the two bacterial species might be due to conformation differences of the bacterial membranes. Gram positive bacteria could have a membrane more susceptible to the AMPs than Gram negative bacteria.

5.2.6 AMP-silks influenced biofilm formation

The CLSM investigation of disks also made it possible to measure biofilm thickness, which was measured at some of the places where pictures were taken for the coverage analyses. The thickness measurements from the several different places of each disks were averaged into two different thickness measurements for each disk; one average for the main layer of biofilm and one average for the thickest clusters of biofilm on each disk. On some of the coated disks, the biofilm formed an even layer, without any clusters. On these disks, measurements were therefore only taken of the main layer. As a consequence, less replicates could be included for analysis of the biofilm thickness at the thickest places of the disks, as there were no such measurements. Therefore, the multicomparison, using Tukey's range test, would be based on too few measurements to show any statistically significant differences between disks, even if there in fact were real differences between them.

The WGR- and Mag-silks showed indications of having the largest inhibitory effect on the *S. aureus* biofilm thickness (Fig. 4.9). If more measurements had been taken on each disks, and most importantly, more replicates had been made from each type of disk, the results from the biofilm thickness analysis would most likely have shown a statistically significant inhibition of biofilm thickness from these AMP-silks.

Incubations of *S.aureus* on the disks were done for 24 and 48 hours. Only 1 ml of TSB growth medium was used for incubation of approximately $5*10^4$ bacteria on each disk, during which the bacteria population continuously grew. Eventually, the TSB medium would run out of nutrients, which would halter bacterial growth. The bacteria population would start to decline as a result of nutrient deprivation and lack of oxygen. This might have contributed to the sometimes lower bacterial coverage and biofilm thickness on disks after 48 hours than after 24 hours (Fig. 4.5–4.9). The natural killing effect due to nutrient deprivation would be biggest where bacteria initially grew most efficiently, which seem to have been on the uncoated disks. The inhibitory effect of the AMP-silks on bacterial coverage and biofim formation on the disks might actually have been greater than results indicated. If the higher concentration of bacteria in samples with uncoated disks depleted nutrient depots faster, they would start to die at a faster rate than in the AMP-silk samples, where concentrations were kept down due to antimicrobial effects of the AMPs. This would level out the differences that could be seen between the coated and uncoated samples, leading to less significant results.

5.2.7 Only the living fractions of bacteria were compared

Only the fractions of living bacteria covering the disks were presented in the results from the disk's surfaces investigations using CLSM (Fig. 4.5, 4.7 and 4.8). The fractions of dead bacteria adhered to the disk's surfaces were low for all disks, which might have been partly due to that dead bacteria more easily got detached during the washing procedure that was performed on the disks prior to investigation. Another reason for the low detection of dead bacteria however, was due to a technical problem with the confocal microscope. The Ne/He laser set to λ_{ex}=594 nm that was used to excite propidium iodide in the dead bacteria was unfortunately not working properly. The signal from the laser was focused on a little section in the middle of the investigated area, and adjusting the signal gain could not correct this. Therefore, the analysis of the amount of dead bacteria on the pictures was not comparable to the amount of living bacteria, since dead bacteria only was visualized in a much smaller section of each analyzed picture. The amount of living bacteria however far exceeded the dead fraction on all analyzed disks, and therefore comparisons between disks were made only on the living fractions.

5.2.8 Weaker adhesion of bacteria on uncoated disks

There was a difference between coated and uncoated disk, that could be seen during investigation of the surfaces using CLSM. Some of the investigated uncoated disks completely lacked adhered bacteria, while on others, the biofilm layer was really thick. Only the uncoated disks which had bacteria adhered to the surfaces were included in results from the CLSM investigation. The same washing procedure on the AMP-silk disks would not leave disks lacking adhered bacteria altogether, which indicated that a distinction could be made between disks that might have lost the biofilm during washing and disks on which adhesion of bacteria was likely inhibited as a result of the coating. The biofilm on the uncoated disks, which seem to have grown thicker than on the coated ones, was likely heavier and therefore more easily washed off, than the biofilms on the coated disks. Also, the spider silk protein coatings might have provided a surface which enabled stronger adhesion of the bacteria than the uncoated polystyrene surface. Therefore, it was concluded that the biofilm was likely washed off during preparation on the uncoated disks that showed no adhered bacteria.

In case of bacteria adhesion on implants, the biofilm would be left undisturbed, since the implant would not be washed after implantation. It seemed more realistic to keep the results only from the uncoated disks that still showed an intact biofilm after the washing procedure, and exclude the disks that lacked adhered bacteria.

5.2.9 Image analysis of investigated disks

The CLSM proved very useful for investigation of the disk's surfaces. The main problem with this method was that some disks did not lay evenly on the microscope cover glass, which made it difficult to maintain focus over the entire investigated surface when capturing micrograpghs of the disks. The signal (gain) from the bacteria was sometimes stronger on some part of the micrograph, which had an effect in the analysis of the images. A stronger signal were translated to a larger coverage of bacteria than a weaker signal, by the analysis software. This could have been corrected for by changing the thresholds for what constituted a bacteria in the analysis software, but would have needed to be done manually for every uneven image. Therefore, micrographs with uneven gains were sorted out during analysis, resulting in fewer measurements on some disks than others. The lowest amount of analyzed images from a single disk was 13, from a Lac disks incubated with *E. coli*. However, mean values of bacterial coverage on each disk were often based on analysis of at least 20 images.

6

Conclusions

All antimicrobial petide silk fusion protein coatings reduced bacterial adhesion of the Gram positive *Staphylococcus aureus* to the polysterene disks after 48 hours. The reduction of bacterial adhesion was likely due to a bactericidal effect of the AMP-silks. A reduction of bacterial adhesion to the disks could be seen from the silk protein itself after the same time, but seemed to be improved by addition of the AMPs. The bactericidal effect of the AMP-silks improved over time, but could be detected on *S. aureus* already after 24 hours for the Mag- and WGR-silk. The WGR-silk had the best bactericidal effect on *S. aureus* after a shorter incubation time, but the other AMP-silks seemed to have equally good bactericidal effect when the incubation time was extended.

The WGR-silk was however ineffective in reducing adhesion of the Gram negative *Escherichia coli* after 24 hours. The only AMP-silk with an antimicrobial effect on *E. coli* after 24 hours was the Mag-silk. However, the spider silk itself might have accounted for this effect, as the addition of the Mag-AMP did not significantly improve the bactericidal effect of the silk on this bacterial species.

In conclusion, the AMP-silks all showed a tendency for antimicrobial activity in a coated state, on Gram positive *S. aureus*. The Mag- and WGR-silks were most effective, where an antimicrobial efffect on *S. aureus* could be seen already after 24 hours. The same antimicrobial effect of the AMP-silks could not be seen on Gram negative *E. coli*, but the spider silk itself seemed to inhibit adhesion of both species of bacteria compared to uncoated polystyrene.

It was also concluded that the WGR-silk could be expressed and purified using a bacterial cloning host, and maintain functionality to form fibers after purification. However, the purification process would need further optimization to improve the yield of purified WGR-silk protein from the bacterial host.

7

Future work

The production of a spider silk biomaterial with an antimicrobial effect is still in the early developmental stage, where studies on biocompability of the AMP-silks are ongoing.

Further studies are also needed on the antimicrobial effect of the AMP-silk coatings on surfaces that are more relevant in medical applications, such as titanium. Ongoing work is being made on coating other materials with recombinant spider silk, which could soon enable studies being made of the AMP-silks coated on a more relevant surface for medical applications than polystyrene.

The silk's ability to form different structures could also enable optimizing the structure of the AMP-silk material for antimicrobial effect. Ultimately, the material should be able to perform an antimicrobial activity on a wide range of infectious bacteria.

A scaled up production of AMP-silk coatings would require the production process to be more effective. More work has to be done in optimizing the expression and purification of the material, trying to find the most efficient conditions during the whole process.

Fortunately, this is work in progress, which will hopefully enable the much needed transition from use of conventional antibiotics to more sustainable options. Antimicrobial silk has the potential to lead development one step closer to that goal.

References

[1] World Health Organization, et al. Antimicrobial resistance: global report on surveillance. World Health Organization; 2014.

[2] Cotter PD, Ross RP, Hill C. Bacteriocins—a viable alternative to antibiotics? Nature Reviews Microbiology. 2013;11(2):95–105.

[3] Gomes SC, Leonor IB, Mano JF, Reis RL, Kaplan DL. Antimicrobial functionalized genetically engineered spider silk. Biomaterials. 2011;32(18):4255–4266.

[4] Liebens V, Gerits E, Knapen WJ, Swings T, Beullens S, Steenackers HP, et al. Identification and characterization of an anti-pseudomonal dichlorocarbazol derivative displaying anti-biofilm activity. Bioorganic & medicinal chemistry letters. 2014;24(23):5404–5408.

[5] Römling U, Balsalobre C. Biofilm infections, their resilience to therapy and innovative treatment strategies. Journal of internal medicine. 2012;272(6):541–561.

[6] Rising A, Widhe M, Johansson J, Hedhammar M. Spider silk proteins: recent advances in recombinant production, structure–function relationships and biomedical applications. Cellular and Molecular Life Sciences. 2011;68(2):169–184.

[7] Widhe M, Hedhammar M, Rising A. Invited review current progress and limitations of spider silk for biomedical applications. Biopolymers. 2012;97(6):468.

[8] Nilebäck L. Recombinant spider silk with antimicrobial properties [diploma thesis on the Internet]. Linköping University. Linköping;. Date accessed: 2016-01-27. Available from: `http://liu.diva-portal.org/smash/get/diva2:685400/FULLTEXT01.pdf`.

[9] Widhe M, Shalaly ND. A fibronectin mimetic motif improves integrin mediated cell biding to recombinant spider silk matrices. Biomaterials. 2016;74:256–266.

[10] Jansson R, Courtin CM, Sandgren M. Rational Design of Spider Silk Materials Genetically Fused with an Enzyme. Advanced Functional Materials. 2015;25(33):5343–5352.

[11] Jansson R, Thatikonda N, Lindberg D, Rising A, Johansson J, Nygren PÅ, et al. Recombinant spider silk genetically functionalized with affinity domains. Biomacromolecules. 2014;15(5):1696–1706.

[12] Zhang F, Zhang Z, Zhu X, Kang ET, Neoh KG. Silk-functionalized titanium surfaces for enhancing osteoblast functions and reducing bacterial adhesion. Biomaterials. 2008;29(36):4751–4759.

[13] Kerr KG, Snelling AM. *Pseudomonas aeruginosa*: a formidable and ever-present adversary. Journal of Hospital Infection. 2009;73(4):338–344.

[14] Hedhammar M, Rising A, Grip S, Martinez AS, Nordling K, Casals C, et al. Structural Properties of Recombinant Nonrepetitive and Repetitive Parts of Major Ampullate Spidroin 1 from Euprosthenops australis: Implications for Fiber Formation†. Biochemistry. 2008;47(11):3407–3417.

[15] Stark M, Grip S, Rising A, Hedhammar M, Engström W, Hjälm G, et al. Macroscopic fibers self-assembled from recombinant miniature spider silk proteins. Biomacromolecules. 2007;8(5):1695–1701.

[16] Fredriksson C, Feinstein R, Nordling K, Kratz G, Johansson J, Huss F, et al. Tissue response to subcutaneously implanted recombinant spider silk: an in vivo study. Materials. 2009;2(4):1908–1922.

[17] Hassan M, Kjos M, Nes I, Diep D, Lotfipour F. Natural antimicrobial peptides from bacteria: characteristics and potential applications to fight against antibiotic resistance. Journal of Applied Microbiology. 2012;113(4):723–736.

[18] Nissen-Meyer J, Nes I. Ribosomally synthesized antimicrobial peptides: their function, structure, biogenesis, and mechanism of action. Archives of Microbiology. 1997;167(2/3):67–77.

[19] Brogden KA. Antimicrobial peptides: pore formers or metabolic inhibitors in bacteria? Nature Reviews Microbiology. 2005;3(3):238–250.

[20] Nguyen LT, Haney EF, Vogel HJ. The expanding scope of antimicrobial peptide structures and their modes of action. Trends in biotechnology. 2011;29(9):464–472.

[21] Bahar AA, Ren D. Antimicrobial peptides. Pharmaceuticals. 2013;6(12):1543–1575.

[22] Gunn J. The Salmonella PmrAB regulon: lipopolysaccharide modiciations, antimicrobial peptide resistance and more. Trends in Microbiology. 2008;16(6):284–290.

[23] Kraus D, Peschel A. *Staphylococcus aureus* evasion of innate antimicrobial defense. Future Microbiology. 2008;3(4):437–451.

[24] Maria-Neto S, de Souza Cândido E, Rodrigues DR, de Sousa DA, da Silva EM, de Moraes LMP, et al. Deciphering the magainin resistance process of Escherichia coli strains in light of the cytosolic proteome. Antimicrobial agents and chemotherapy. 2012;56(4):1714–1724.

[25] Zhang LJ, Gallo RL. Antimicrobial peptides. Current Biology. 2016;26(1):R14–R19.

[26] Humblot V, Yala JF, Thebault P, Boukerma K, Héquet A, Berjeaud JM, et al. The antibacterial activity of Magainin I immobilized onto mixed thiols Self-Assembled Monolayers. Biomaterials. 2009;30(21):3503–3512.

[27] Pedrosa M, Mouro C, Nogueira F, Vaz J, Gouveia I. Comparison of the antibacterial activity of modified-cotton with magainin I and LL-37 with potential as wound-dressings. Journal of Applied Polymer Science. 2014;131(21).

[28] Kim HK, Chun DS, Kim JS, Yun CH, Lee JH, Hong SK, et al. Expression of the cationic antimicrobial peptide lactoferricin fused with the anionic peptide in Escherichia coli. Applied microbiology and biotechnology. 2006;72(2):330–338.

[29] Schmidtchen A, Pasupuleti M, Mörgelin M, Davoudi M, Alenfall J, Chalupka A, et al. Boosting antimicrobial peptides by hydrophobic oligopeptide end tags. Journal of Biological Chemistry. 2009;284(26):17584–17594.

[30] Zasloff M, Martin B, Chen HC. Antimicrobial activity of synthetic magainin peptides and several analogues. Proceedings of the National Academy of Sciences. 1988;85(3):910–913.

[31] Matsuzaki K, Harada M, Handa T, Funakoshi S, Fujii N, Yajima H, et al. Magainin 1-induced leakage of entrapped calcein out of negatively-charged lipid vesicles. Biochimica et Biophysica Acta (BBA)-Biomembranes. 1989;981(1):130–134.

[32] Nascimento JM, Franco OL, Oliveira MD, Andrade CA. Evaluation of Magainin I interactions with lipid membranes: An optical and electrochemical study. Chemistry and physics of lipids. 2012;165(5):537–544.

[33] Glinel K, Jonas AM, Jouenne T, Leprince J, Galas L, Huck WT. Antibacterial and antifouling polymer brushes incorporating antimicrobial peptide. Bioconjugate chemistry. 2008;20(1):71–77.

[34] Lönnerdal B, Iyer S. Lactoferrin: molecular structure and biological function. Annual review of nutrition. 1995;15(1):93–110.

[35] Jenssen H. Antimicrobial Activity of Lactoferrin and Lactoferrin Derived Peptides. Nova Science Publishers, Inc.; 2009.

[36] Dutta D, Kumar N, DP Willcox M. Antimicrobial activity of four cationic peptides immobilised to poly-hydroxyethylmethacrylate. Biofouling. 2016;32(4):429–438.

[37] Schmidtchen A, Ringstad L, Kasetty G, Mizuno H, Rutland MW, Malmsten M. Membrane selectivity by W-tagging of antimicrobial peptides. Biochimica et Biophysica Acta (BBA)-Biomembranes. 2011;1808(4):1081–1091.

[38] Stewart PS, Costerton JW. Antibiotic resistance of bacteria in biofilms. The lancet. 2001;358(9276):135–138.

[39] Breidenstein EB, de la Fuente-Núñez C, Hancock RE. Pseudomonas aeruginosa: all roads lead to resistance. Trends in microbiology. 2011;19(8):419–426.

[40] van de Velde F, Weinbreck F, Edelman MW, van der Linden E, Tromp RH. Visualisation of biopolymer mixtures using confocal scanning laser microscopy (CSLM) and covalent labelling techniques. Colloids and Surfaces B: Biointerfaces. 2003;31(1):159–168.

[41] Carter P, Bedouelle H, Winter G. Improved oligonucleotide site-directed mutagenesis using M13 vectors. Nucleic Acids Research. 1985;13(12):4431–4443.

[42] Lee DG, Urbach JM, Wu G, Liberati NT, Feinbaum RL, Miyata S, et al. Genomic analysis reveals that Pseudomonas aeruginosa virulence is combinatorial. Genome biology. 2006;7(10):R90.

[43] O'Neill, AJ. Staphylococcus aureus SH1000 and 8325-4: comparative genome sequences of key laboratory strains in staphylococcal research. Letters in applied microbiology. 2010;51(3):358–361.